Nuclear Science and Techniques (2026) 37:72
https://doi.org/10.1007/s41365-026-01882-w

Optically stimulated luminescence and thermoluminescence in newly developed $LiMgPO_4$:Gd

Kai-Yong Tang[1,2] · Li Fu[1] · Si-Yuan Zhang[1] · Hai-Jun Fan[1] · Yan Zeng[1,3] · Mo Zhou[1]

Received: 26 June 2024 / Revised: 14 September 2024 / Accepted: 21 September 2024 / Published online: 3 February 2026

Abstract

Five samples of $LiMgPO_4$:Gd were prepared via five different production processes using a solid-state reaction method. The effects of the preparation process on optically stimulated luminescence (OSL) and thermoluminescence (TL) were investigated. Considering its high sensitivity, low fading, and minimum detectable dose (MDD), the $LiMgPO_4$:Gd phosphor heated to 900 °C for 15 h is concluded to be optimal. The effects of annealing on the OSL sensitivity, relative residual OSL signals measured after 24 h of irradiation, and MDD of $LiMgPO_4$:Gd phosphors heated to 900 °C for 15 h were also investigated. Considering its high sensitivity, low fading, and MDD, annealing at 350 °C for 1 h is concluded to be optimal. The OSL signal of $LiMgPO_4$:Gd was derived from the principal TL glow peak. For a maximum integration time of 5 s, the OSL signal was stable, with no fading 30 days after irradiation. $LiMgPO_4$:Gd eliminated approximately 2.2% of the OSL signal at each readout for a readout time of 0.1 s, which is sufficient for fast and multiple OSL readout. The sensitivity of $LiMgPO_4$:Gd phosphor, annealed for 1 h at 350 °C with a reading time of 0.1 s, was found to be approximately 98% of that observed for α-Al_2O_3:C(TLD-500k), which should be sufficient for low-dose measurements in personal, workplace, and environmental dosimetry.

Keywords Fading · $LiMgPO_4$:Gd · Optically stimulated luminescence · Phosphors · Thermoluminescence

1 Introduction

Optically stimulated luminescence (OSL) or thermoluminescence (TL) refer to phenomena whereby a material previously subjected to irradiation releases a luminescent signal in response to the application of an appropriate optical or thermal stimulus [1–4]. TL is a well-established technology that is widely used in various dosimetric applications. These include personal, workplace, and environmental dosimetry; medical dosimetry; imaging of ionizing radiation; archeological and geologic dating; and assessment of radiation accidents [1, 5]. Currently, thermoluminescent dosimeters (TLDs) are predominantly used to assess individual radiation exposure [6–8]. LiF:Mg, Cu, P (GR-200A) is the most prominent example of this approach [9–13].

The basic principles of TL and OSL methods are the same except that the former uses heat to read the signal, whereas the latter uses light stimulation to read the signal [14]. The distinctive stimulation patterns associated with the TL and OSL methods provide the latter with certain advantages [2, 15]. A major advantage of the OSL method over the TL method is the ability to read signals at room temperature without heating the detector. The dosimeters can be used in combination with plastic adhesives at room temperature. In the OSL mode, the intensity of the excitation light and the excitation time can be controlled to read out only a portion of the signal at a time [14]. This is in contrast to the TL mode, in which all signals are read simultaneously. It is possible to perform multiple readout sessions and achieve a rapid readout by reading only a portion of the signal simultaneously. In the InLight reader, each detector was stimulated for a duration of 1 s. To provide multiple readings, a percentage of the OSL

✉ Kai-Yong Tang
13121370921@163.com

1 State Key Laboratory of NBC Protection for Civilian, P.O. Box 1044, Ext. 203, Beijing 102205, China

2 Solid Dosimetric Detector and Method Laboratory, P.O. Box 1044, Ext. 203, Beijing 102205, China

3 School of Materials Science and Engineering, Shanghai University, Shanghai 200444, China

signal was discharged with weak stimulation, with a value of only 0.07%. In contrast, a value of 0.25% was obtained with strong stimulation [14]. Recently, several Individual Monitoring Service (IMS) laboratories have transitioned from using TLD-to-OSL dosimeters [16].

In view of the benefits offered by OSL technology, numerous research teams have addressed the development of new OSL materials; however, only two commercially available OSL dosimeters based on Al_2O_3:C and BeO have been reported. In contrast, the number of TL dosimeters is significantly higher [1]. Interestingly, α-Al_2O_3:C is an ideal OSL material with high stability and sensitivity. Many methods have been adopted to prepare α-Al_2O_3:C OSL dosimeters; however, only α-Al_2O_3:C OSL dosimeters prepared using crystal growth technology have the highest OSL sensitivity [17–22]. The growth of carbon-doped alumina crystals is susceptible to fluctuations in the growth conditions, which can result in considerable variations in the properties of α-Al_2O_3:C detectors between samples and batches [14]. To enhance the uniformity of OSL dosimeters, commercially available Luxel+ and InLight OSL dosimeters were manufactured by blending α-Al_2O_3:C powders with polyester and depositing them on a transparent polyester film [14]. This resulted in the initial dose of the linear range of the dose response of the product being worse than that of the material itself. It has been reported that BeO exhibits a pronounced exponential decline in sensitivity upon initial use [23], accompanied by signal fading following radiation exposure [24].

Many countries are developing novel and enhanced OSL materials. Many materials with OSL properties have been reported [25–29]. However, they have not been widely adopted in commercially available dosimeters because of different inherent limitations. One of them is high fading. In particular, the high fading exhibited by OSL materials used in personal dosimetry and environmental monitoring applications is unacceptable because it inevitably leads to substantial dosimetry inaccuracies. The minimal dose of detectable $Li_2B_4O_7$:Ag is as low as 15 µGy; however, its CW-OSL signal decreased by approximately 30% over a 24-h period after irradiation [30]. Following one day of radiation exposure, the OSL signals of $CaSO_4$:Dy exhibited a decay of approximately 50%, whereas those of $CaSO_4$:Eu exhibited a decay of approximately 10% [31, 32]. The OSL signals from Mg_4SiO_4:Tb and $LiAl_2O_4$:Tb exhibited a decline in intensity between 30% and 40%, spanning approximately 20 h [33]. In a study on $NaMgF_3$ doped with Ce, Tm, and Tb, the OSL response decreased by 20%, 13%, and 35%, respectively, after irradiation for 1 d, 60 h, and 5 d [34, 35]. The minimum detectable doses (MDDs) for MgO:Li,Ce, and Sm are found to be as low as 0.2 µGy. However, a 15% fading in the OSL signals was observed within the initial hour [36].

$LiMgPO_4$ is one of the numerous new OSL materials with excellent dosimetric properties that have been investigated by research teams worldwide [26, 37–50]; however, its main drawback is high fading. A recent study summarized the OSL fading behavior of $LiMgPO_4$. Various conditions, including changes in the dopant species, impurity concentrations, preparation processes, and prereadouts to eliminate the effects of low-temperature peaks, have been used to minimize the fading of $LiMgPO_4$ phosphors. It has been observed that fading can be reduced by preheating or optical treatment. However, the application of preheating or optical treatment resulted in a significant reduction in OSL intensity, with a reduction of 60% to 70% [51]. Similarly, the fading of $LiMgPO_4$:Tb, Sm, B was reduced from 30% without pretreatment to approximately 7% by preheating at 160 °C for 30 s after 30 days of irradiation [52].

One day after irradiation, the fading of $LiMgPO_4$ doped with B alone was reduced from 15% to 30% for $LiMgPO_4$:Tb, B [53]. The low-temperature peak of $LiMgPO_4$:B is still very high, and the fading is still unable to meet the requirements of personal dose monitoring. By varying the preparation temperature, the fading of the $LiMgPO_4$:Tb, Sm, and B phosphors was significantly reduced. The residual OSL signal was as high as 92.3% after 24 h of irradiation [47].

The fading of the OSL signals in $LiMgPO_4$:Er after irradiation has been reported to be reduced by improving the preparation process [41]. It was found that the fading of $LiMgPO_4$:Er samples heated to 900 °C for 10 h was less than 5%, which was observed within 30 d after irradiation when the integration time was greater than or equal to 20 s. However, the fading was greater than 5% when the integration time was less than 20 s.

To gain insight into the features of energy transfer in doped $LiMgPO_4$, $LiMgPO_4$:RE (RE–Nd, Sm, Gd, Tb, Dy, Ho, Er, Tm) was synthesized [39]. Both $LiMgPO_4$:Er and $LiMgPO_4$:Gd exhibit broad emission bands at 360 nm in their TL spectra, and the intensity of the latter is higher than that of the former [39]. However, the OSL characteristics of $LiMgPO_4$:Gd were not studied.

Significant efforts have been made to develop new OSL materials with properties comparable to those of Al_2O_3:C, including a simple synthetic process, easily available raw materials, low cost, and suitability for mass production. The main aim of this study was to improve the time stability of the OSL signal of $LiMgPO_4$ to achieve fast and multiple OSL readouts. Five samples of $LiMgPO_4$:Gd phosphor powder were prepared using five different preparation methods.

The effects of the preparation process on the OSL decay curves, TL glow curves, OSL sensitivity, MDD, and fading characteristics of $LiMgPO_4$:Gd phosphors after 24 h of irradiation were investigated. The impact of annealing on the OSL sensitivity, relative residual OSL signals measured

after 24 h of irradiation, and MDD of $LiMgPO_4$:Gd phosphors heated to 900 °C for 15 h were also investigated. The fundamental characteristics of $LiMgPO_4$:Gd annealed at 350 °C for one hour were examined.

2 Materials and methods

2.1 Material

A simple solid-state reaction method was used to synthesize $LiMgPO_4$:Gd materials. The following reagents were weighed according to a stoichiometric ratio of Li_2CO_3 (lithium carbonate, 99.99%), $3MgCO_3 \cdot Mg(OH)_2 \cdot 3H_2O$ (magnesium carbonate, 99.9%), and $NH_4(H_2)PO_4$ (ammonium dihydrogen phosphate, 99.99%) thoroughly mixed. An appropriate quantity (0.25 mol%) [39] of Gd_2O_3 was added to the mixture, which was then mixed thoroughly.

Five distinct processes were employed to prepare the $LiMgPO_4$:Gd phosphors. The synthesis of the $LiMgPO_4$:Gd phosphor was divided into three stages. The two initial stages of the five preparatory processes for $LiMgPO_4$:Gd were identical, with only the third stage differing. In the first phase of the procedure, the mixture was placed in an alumina crucible and pushed into the center of the tube furnace. It was then heated from room temperature to 300 °C for 30 min, after which it was maintained at 300 °C for 2 h. The crucible was then removed from the furnace and rapidly cooled to room temperature. The samples were manually pulverized and sieved. In the second step, the material obtained in the first step was subjected to a temperature increase from 300 to 650 °C for 30 min, after which it was maintained at 650 °C for 2 h. The third step of the first three preparations involved heating the material obtained in the second step from 650 to 900 °C for 30 min. This was followed by additional periods of 10, 15, or 20 h at 900 °C, respectively. In the third step of the preparation process for 4 and 5, the material obtained in the second step was heated from 650 to 950 °C and 1000 °C, respectively, for 30 min, and then maintained at 950 °C and 1000 °C for 2 h, respectively.

For comparison, an α-Al_2O_3:C detector (TLD-500K) with a 5 mm diameter and 0.9 mm thickness was used.

2.2 Characterizations

The powder structure was characterized by powder X-ray diffraction (XRD; Bruker D8 Advance). Scanning electron microscopy (SEM) and energy-dispersive spectroscopy (EDS) were performed to confirm the presence of Gd in the structure using a Hitachi SU8600.

The Risø TL/OSL reader TL/OSL-DA-20 was used to measure the OSL decay curves and TL glow curves of the samples, as well as the β-source irradiation. Many studies have been published on this TL/OSL reader; therefore, it will not be described in detail here [41, 52]. A continuous-wave OSL (CW-OSL) method was used for OSL measurements. The stimulus power was 90% and the duration was 88 s. TL glow curves were measured from room temperature to 450 °C at a heating rate of 5 °C s^{-1}.

To test the effect of the preparation process on the OSL decay curves, TL glow curves, OSL sensitivity, MDD, and fading characteristics of the $LiMgPO_4$:Gd phosphors, the five types of samples for the five preparation processes were fully bleached using the TL readout method, which involves pretreatment at a ramp rate of 5 °C per second, followed by a readout temperature of 450 °C; then, their OSL background signals were measured. A $^{90}Sr/^{90}Y$ β source was used to irradiate the samples for 2 s at a nominal dose rate of 50 µGy s^{-1} to measure the OSL decay curve, TL glow curve, and fading signal 24 h after irradiation.

To ascertain the effect of annealing temperature on the OSL sensitivity, MDD, and fading of $LiMgPO_4$:Gd 24 h after irradiation, $LiMgPO_4$:Gd powders synthesized at 900 °C for 15 h were subjected to annealing treatment at temperatures between 350 °C and 500 °C at intervals of 50 °C for an hour. The background signal was quantified immediately following the annealing of the samples, which were subjected to irradiation at ambient temperature for 2 s at a nominal dose rate of 50 µGy s^{-1} using a $^{90}Sr/^{90}Y$ β source integrated into the Risø reader. Subsequently, OSL signals were recorded. The samples were fully bleached using the TL readout method, which entailed a pretreatment with a temperature ramp rate of 5 °C s^{-1}, followed by a readout to 450 °C, and then irradiated at ambient temperature using a $^{90}Sr/^{90}Y$ β source integrated into the Risø reader at a nominal dose rate of 50 µGy s^{-1} for 2 s. Subsequently, the OSL signal was recorded 24 h after irradiation.

To experimentally assess the long-term fading of $LiMgPO_4$:Gd, a sample of $LiMgPO_4$:Gd synthesized at 900 °C for 15 h was used. Before irradiation, the samples were annealed at 350 °C for one hour. To investigate the kinetic order of $LiMgPO_4$:Gd, the samples were completely bleached. This involved pretreatment at a rate of 5 °C per second, followed by a readout temperature of 450 °C, irradiation with a dose of 0.1 Gy using a β-in situ irradiator, and subsequent reading of the TL glow curves at 450 °C. The heating rate of the TL readings was set to 5 °C s^{-1}, and this was repeated six times at irradiation doses of 0.2, 0.5, 1, 2, 5, and 10 Gy.

To experimentally assess the long-term fading of $LiMgPO_4$:Gd, the sample was irradiated with a dose of 50 µGy from a ^{60}Co gamma source. The OSL signals were read at 0 days (approximately 40 min) and 1, 2, 5, 10, 20, and 30 days after irradiation.

To study the reusability of $LiMgPO_4$:Gd, five samples of $LiMgPO_4$:Gd, each weighing 10 mg, were extracted and placed at five distinct positions within the TL/OSL reader. The samples were fully bleached using the TL readout method, which entailed a pretreatment with a temperature ramp rate of 5 °C per second, followed by a readout to 450 °C, and then irradiated at ambient temperature using a (90Sr)/90 Y β source integrated into the Risø reader at a nominal dose rate of 50 μGy s^{-1} for 2 s before reading out the OSL signal; ten such cycles were performed.

3 Results

3.1 X-ray diffraction (XRD)

Figure 1 shows the XRD patterns of $LiMgPO_4$:Gd samples produced through five distinct preparation processes in conjunction with Inorganic Crystal Structure Database (ICSD) Card No. 201138. The measured diffraction patterns agreed with the reference pattern with respect to the positions of the majority of reflections. However, the differences in sensitivity may also be attributable to variations in sample preparation.

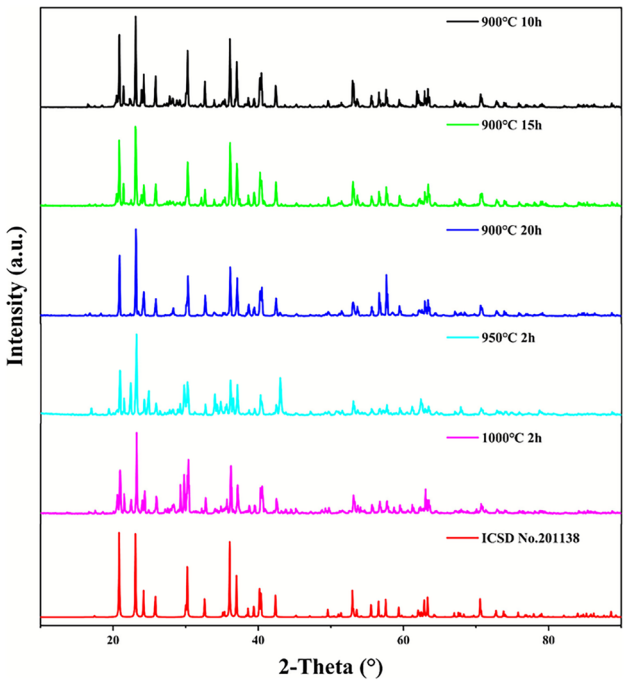

Fig. 1 (Color online) XRD patterns of the $LiMgPO_4$:Gd samples produced by five preparation processes and Inorganic Crystal Structure Database (ICSD) Card No. 201138

3.2 Elemental analysis

Figure 2 depicts the map sum spectra of LiMgPO4:Gd samples produced using five distinct preparation processes. Figure 2 illustrates the presence of gadolinium in the structure.

3.3 Effect of preparation processes

The effects of the five preparation processes on $LiMgPO_4$:Gd phosphors are shown in Fig. 3. The OSL decay curves, normalized by the maximum of the $LiMgPO_4$:Gd phosphors produced using the five preparation processes, are shown in Fig. 3a. The $LiMgPO_4$:Gd phosphor heated to 900 °C for 15 h exhibited the slowest decay. In contrast, the $LiMgPO_4$:Gd phosphor heated to 1000 °C for 2 h exhibited the fastest decay. The remaining three curves exhibit relatively similar decay profiles.

The normalized OSL signals of the five $LiMgPO_4$:Gd phosphors prepared by the five processes, compared to TLD-500k for various integration times, are shown in Fig. 3b. The OSL signals were averaged over five readings for each data point. All standard deviations were less than 10%. Note that the OSL signals of the $LiMgPO_4$:Gd phosphors from the five preparation processes are lower than those of the TLD-500k phosphors for the different integration times. The highest OSL sensitivity was obtained for the $LiMgPO_4$:Gd phosphor heated to 900 °C for 15 h.

The relative residual OSL signals of the five $LiMgPO_4$:Gd phosphors prepared using the five preparation methods with different integration times measured after 24 h of irradiation compared to those measured immediately after irradiation are shown in Fig. 3c. The OSL signals were averaged over five readings for each data point. For the sample heated to 1000 °C for 2 h, the relative residual OSL signals measured after 24 h of irradiation were approximately 0.701−0.88, while the relative residual OSL signals measured after 24 h of irradiation for the other four samples were stable for the different integration times.

The OSL MDDs of the five $LiMgPO_4$:Gd phosphors prepared using the five processes are presented in Fig. 3d. The preparation process has a significant impact on the MDD. Relatively low MDDs were observed in the samples heated to 950 °C for 15 h and different integration times.

Typical TL glow curves and TL integrated signals of the five $LiMgPO_4$:Gd phosphors prepared using the five processes are presented in Fig. 3e and 3f. For clarity, Fig. 3e shows the TL signal between 50 °C and 300 °C because of the minimum TL signal between 300 °C and 450 °C. The $LiMgPO_4$:Gd phosphor heated to 900 °C for 15 h exhibited the highest TL sensitivity. In contrast, the $LiMgPO_4$:Gd phosphor heated to 1000 °C for 2 h exhibited the lowest TL sensitivity.

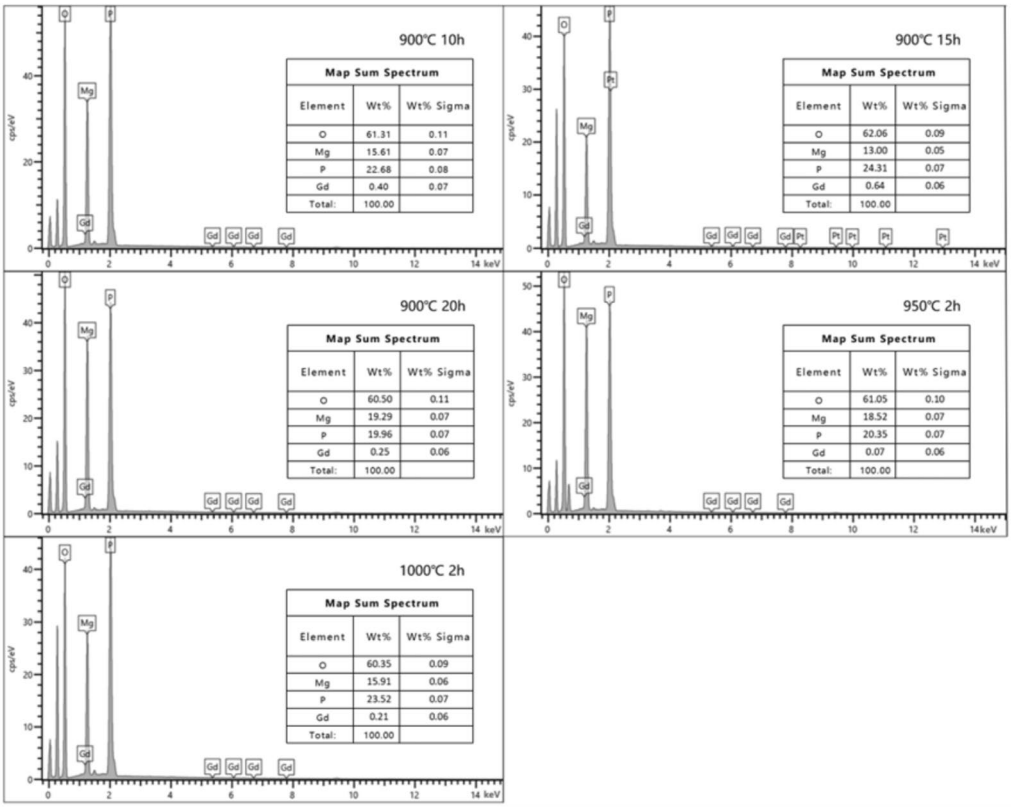

Fig. 2 Map sum spectra of the $LiMgPO_4$:Gd samples produced by five preparation processes

Considering its high sensitivity, low fading, and MMD, the $LiMgPO_4$:Gd phosphor heated to 900 °C for 15 h is concluded to be optimal. The following study is conducted only on the $LiMgPO_4$:Gd phosphor.

3.4 Effect of annealing on $LiMgPO_4$:Gd

The effect of annealing on $LiMgPO_4$:Gd phosphors is shown in Fig. 4. Figure 4a shows the OSL signals of four distinct types of $LiMgPO_4$:Gd phosphors, each subjected to annealing processes at temperatures of 350, 400, 450, and 500 °C for 1 h. The single unannealed $LiMgPO_4$:Gd phosphor was normalized to TLD-500k at various integration times. Each data point in the figure corresponds to the mean value of the OSL signals for the five samples. The standard deviations of these values were less than 10%. The OSL sensitivity of $LiMgPO_4$:Gd can be enhanced by annealing. The $LiMgPO_4$:Gd phosphor annealed at 350 °C for 1 h exhibited the highest OSL sensitivity. It is observed that as the annealing temperature exceeds 350 °C, the OSL sensitivity decreases by the rise in annealing temperature. The initial and total OSL signals were found to be essentially identical to those of TLD-500k at an annealing temperature of 350 °C. The initial OSL signal of the $LiMgPO_4$:Gd phosphor annealed for 1 h at 350 °C relative to that of TLD-500k was approximately 0.98.

Figure 4b depicts the relative residual OSL signals after 24 h of the irradiation to the signals immediately after irradiation for four distinct types of $LiMgPO_4$:Gd phosphors annealed at 350, 400, 450, and 500 °C for 1 h, and a single unannealed $LiMgPO_4$:Gd phosphor. The highest residual OSL signal was observed for the unannealed phosphor. For annealed phosphors, the OSL signal can be considered stable when the integration time is less than 10 s.

Figure 4c depicts the OSL MDD for four distinct types of $LiMgPO_4$:Gd phosphors annealed at 350, 400, 450, and 500 °C for 1 h, and a single unannealed $LiMgPO_4$:Gd phosphor. The OSL MDD of $LiMgPO_4$:Gd was significantly reduced by annealing. The OSL MDD of $LiMgPO_4$:Gd phosphors annealed for one hour at 350 °C was as low as 2.2 μGy when the integration time was one second, and 16.2 μGy when the integration time was 0.1 s.

Considering the high sensitivity, low fading, and MDD, annealing the $LiMgPO_4$:Gd phosphor at 350 °C for 1 h was optimal. The following study is conducted only on the $LiMgPO_4$:Gd phosphor.

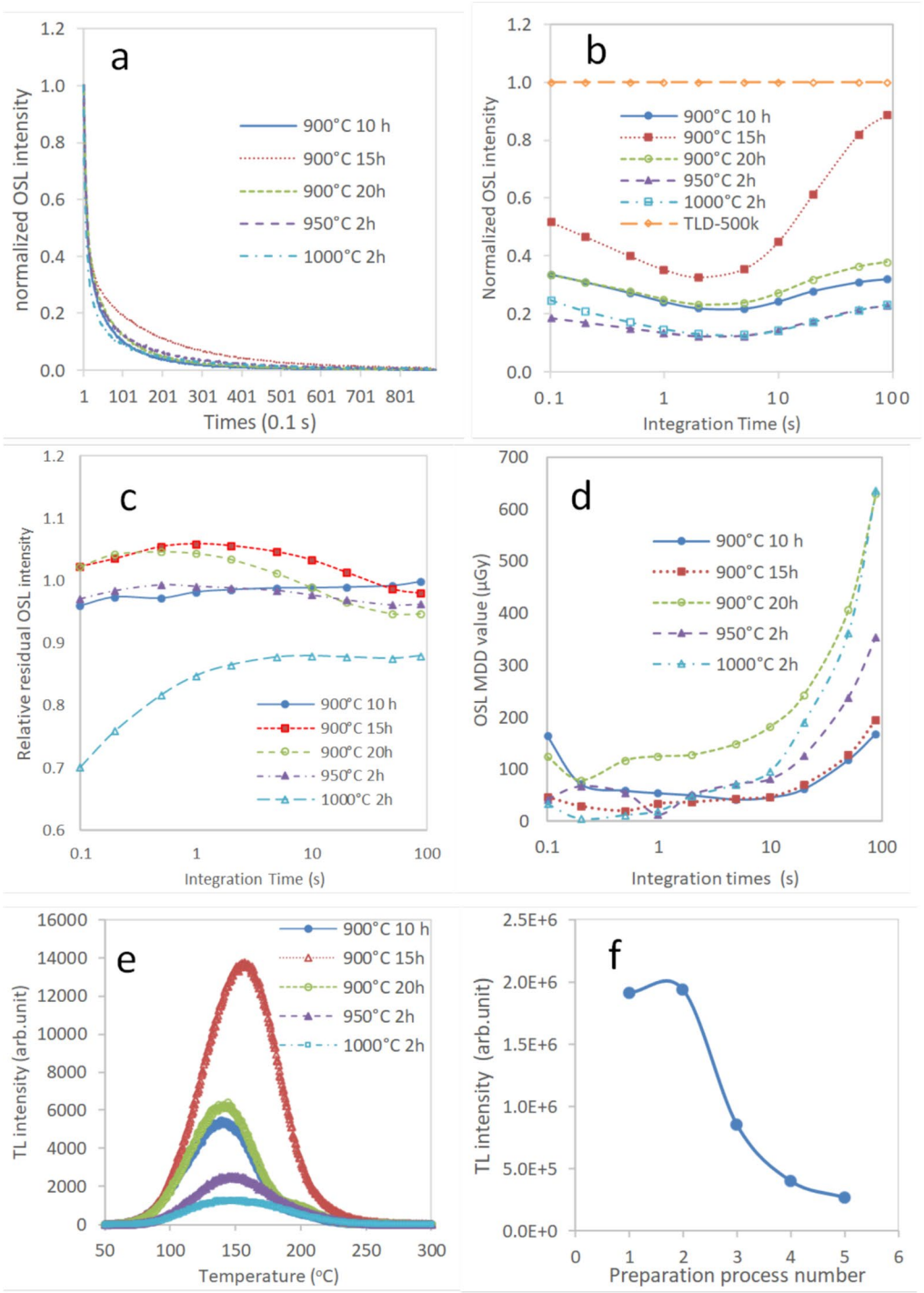

Fig. 3 (Color online) Effect of five preparation processes on $LiMgPO_4$:Gd phosphors

3.5 Basic properties of $LiMgPO_4$:Gd

3.5.1 TL dose response and kinetic order

The effects of dose, heating rate, and OSL readings on the TL of the $LiMgPO_4$:Gd phosphor and OSL decay curve are shown in Fig. 5. In Fig. 5a, the glow curves for the $LiMgPO_4$:Gd phosphors were recorded under irradiation conditions of 0.1–10 Gy; the phosphors were initially maintained at room temperature and subsequently heated to 450 °C at a constant rate of 5 °C s^{-1}. For clarity, Fig. 5a shows the TL signal between 50 °C and 250 °C, because of

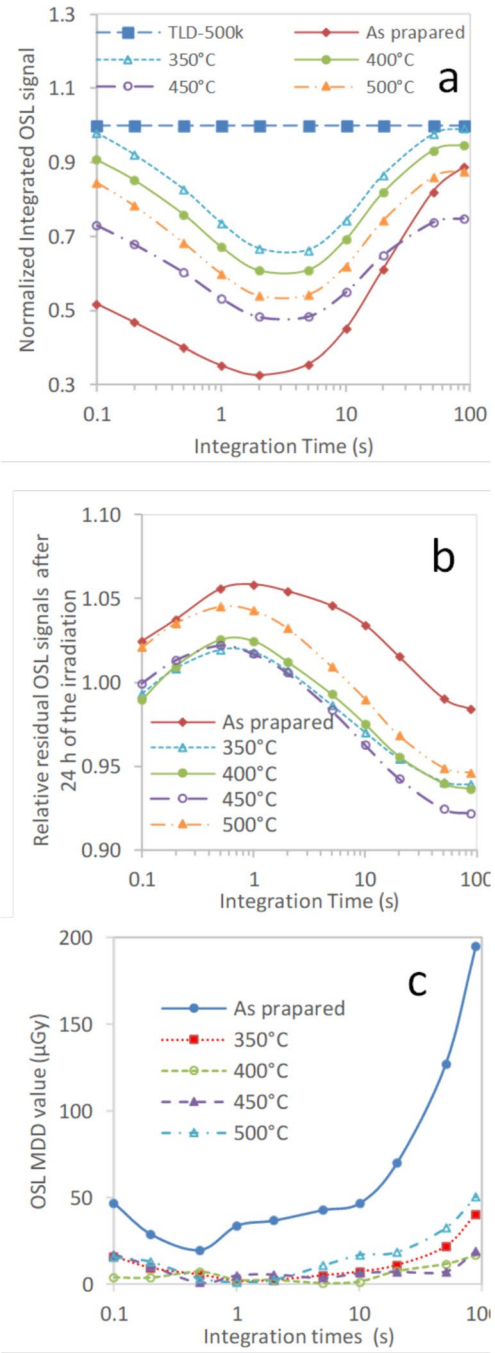

Fig. 4 (Color online) Effect of annealing on $LiMgPO_4$:Gd phosphors

the minimum TL signal between 450 °C and 450 °C. The peak temperature of $LiMgPO_4$:Gd was found to be consistently positioned at 131.4 ± 1.1 °C for varying irradiation doses. The peak shift method [5] indicates that the peak of the TL glow curve in the $LiMgPO_4$:Gd phosphor represents a first-order phenomenon because the temperature at which the peak occurs remains constant. The dose responses of the $LiMgPO_4$:Gd phosphors are shown in Fig. 4b. Over the investigated dose range of 0.1–10 Gy, the $LiMgPO_4$:Gd phosphors exhibited an excellent linear response (Fig. 5b).

3.5.2 TL kinetics parameters

Figure 5c shows five glow curves for the $LiMgPO_4$:Gd phosphors that were evaluated and recorded at ramping rates of 0.2 to 5 °C s^{-1}. The samples were irradiated with 0.1 Gy and subjected to an increase in temperature from room temperature to 450 °C. For clarity, the TL signal between 50 and 250 °C is shown in Fig. 4c, because of the minimum TL signal between 250 °C and 450 °C. As the heating rate increased from 0.5 °C s^{-1} to 5 °C s^{-1}, the peak temperature gradually increased and the peak and total integral TL signals decreased.

The variable heating rate (VHR) method [5] was used to obtain the kinetic parameters of the peaks in the glow curve. This method requires only peak temperature information. Therefore, it can be applied to peaks with well-defined peak temperatures. However, this method can only be applied to peaks with first-order kinetics. The kinetic parameters of $LiMgPO_4$:Gd can be obtained using the VHR method because the peak of the TL glow curve in this sample appears to be a first-order phenomenon.

The theory of TL kinetics proposes that in first-order kinetics, the following relationship exists between the peak temperature (T_m) and heating rate (β) [54]:

$$\ln\left(\frac{T_m^2}{\beta}\right) = \left(\frac{1}{kT_m}\right)E + \ln\left(\frac{E}{sk}\right), \quad (1)$$

where E is the activation energy, k is the Boltzmann constant, and s is the pre-exponential factor.

When plotting the natural logarithm of T_m^2/β against $1/(T_m)$, a line with a slope of E/k and an intercept of $\ln(E/ks)$ is obtained. This enables the calculation of the E and s parameters. The representation of $\ln(T_m^2/\beta)$ versus $1/(T_m)$ for the $LiMgPO_4$:Gd samples is shown in Fig. 5d. The E and s values calculated using Eq. (1) and Fig. 5d were 1.44 eV and 4.82×10^{17} s^{-1}, respectively.

3.5.3 TL after OSL

Figure 5e shows a comparison between the measured TL glow curve immediately following radiation exposure and the TL glow curve following the OSL readout. The peak height of the TL glow curve of the $LiMgPO_4$:Gd sample measured immediately was approximately 14 times greater than that of the TL glow curve measured after the use of OSL. The total area of the TL peak after the OSL measurements was 8.5% of the area recorded immediately after irradiation over a temperature range of 50 – 250 °C. It can be observed that the OSL signal present in $LiMgPO_4$:Gd

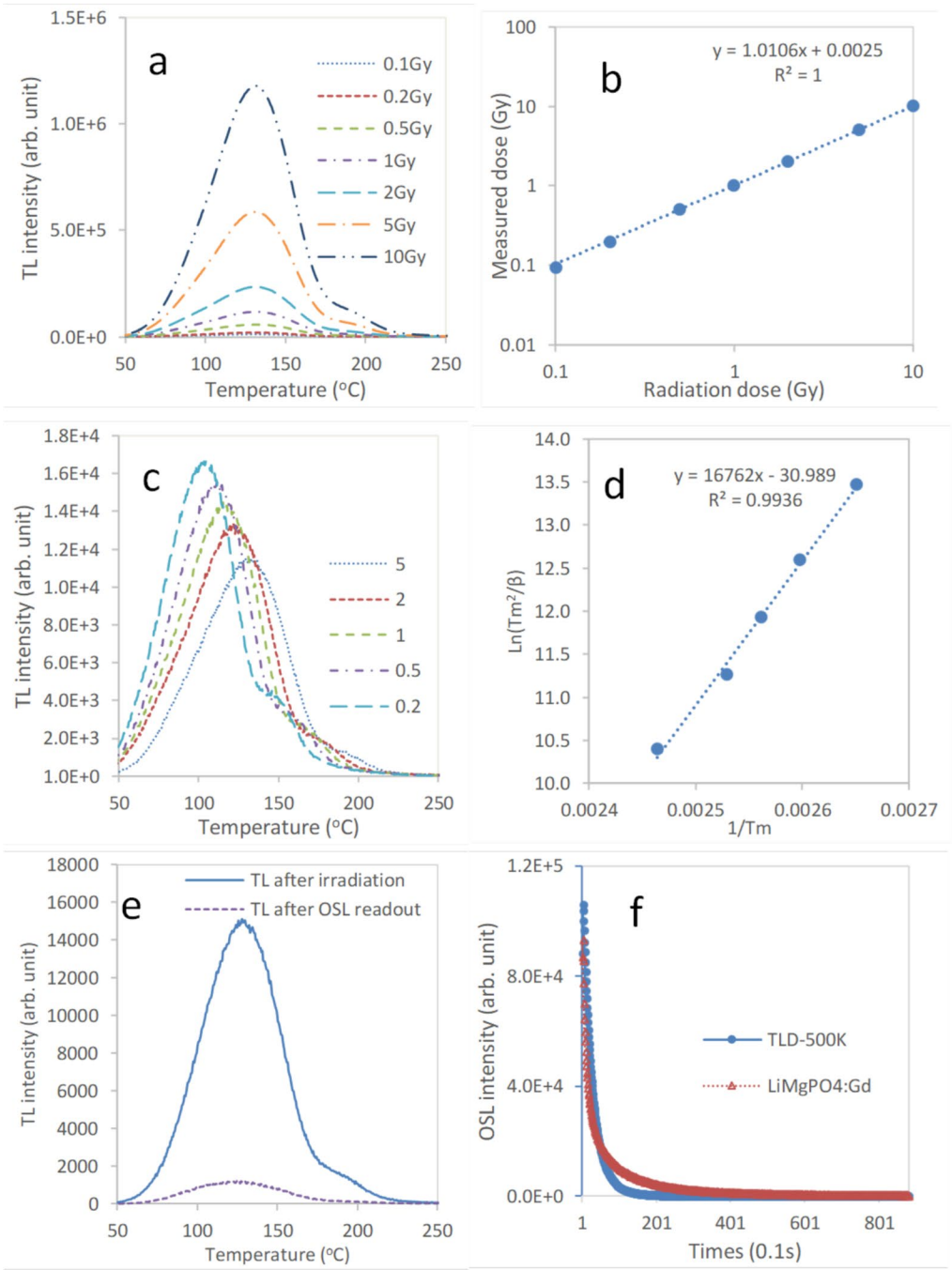

Fig. 5 (Color online) Effects of dose, heating rate, and OSL readings on the TL of the $LiMgPO_4$:Gd phosphor

is derived from the principal TL glow peak. Furthermore, the majority of traps that lead to this signal can be eliminated using OSL readings.

3.5.4 OSL decay curve

The decay curves per unit mass for $LiMgPO_4$:Gd and TLD-500k are compared in Fig. 5f. As the measurement time increased, $LiMgPO_4$:Gd began to decrease faster and then TLD-500k decreased faster. Therefore, the sensitivity of $LiMgPO_4$:Gd relative to that of TLD-500k decreased and then increased as the measurement time increased. During this investigation, the elimination of approximately 2.2% and 2.9% of the OSL signals, respectively, was observed in the case of $LiMgPO_4$:Gd and TLD-500k following each readout at a readout time of 0.1 s.

3.5.5 OSL long-term fading

Table 1 presents the relative residual OSL signals of the $LiMgPO_4$:Gd phosphors as functions of time after irradiation and integration time. For a maximum integration time of 5 s, the OSL signal was stable, with no fading 30 days after radiation exposure. The data points represent the mean values of the OSL signals obtained from five aliquots.

3.5.6 Reusability

Table 2 presents the repeatability of the normalized OSL signals for the $LiMgPO_4$:Gd phosphors with different integration times. The coefficient of variation for the repeated cycles of the $LiMgPO_4$:Gd samples at different integration times was less than 0.8%, demonstrating the excellent reproducibility of the powders.

4 Discussion

4.1 Sensitivity

The sensitivity of OSL materials to radiation is one of their most important properties. Low doses must be measured in personal, workplace, and environmental dosimetry, and OSL materials must have high sensitivity. The sensitivity and MDD of integrated passive detectors for personal, workplace, environmental photon, and beta radiation monitoring are not specified in the IEC 62387 standard. Instead, they only correspond to the dose linearity floor of the entire dosimetry system, which is mandatory at 0.1 mSv. However, to assess the sensitivity of a novel material, it is common practice to compare the response signal of such a material with that of a well-known material used commercially in dosimetry systems [1], measured under identical conditions.

The two principal advantages of OSL dosimetry over TL dosimetry are the speed of readout and the capacity for multiple readouts. The former enhances the processing capacity of many dosimeters, whereas the latter safeguards against

Table 1 Normalized intensities of $LiMgPO_4$:Gd specimens at different measurement times after exposure to radiation over different integration periods. Each value represents the average response of the five aliquots

Integration time (s)	0 day	1 day	2 days	5 days	10 days	20 days	30 days
0.1	1.000	1.000	1.007	0.994	0.985	0.972	0.979
0.2	1.000	1.004	1.013	1.009	1.007	0.981	1.011
0.5	1.000	1.004	1.013	1.018	1.022	1.024	1.037
1	1.000	1.000	1.006	1.012	1.021	1.036	1.036
2	1.000	0.992	0.996	1.000	1.008	1.028	1.018
5	1.000	0.978	0.977	0.973	0.973	0.998	0.972
10	1.000	0.962	0.955	0.941	0.932	0.965	0.921
20	1.000	0.940	0.926	0.904	0.883	0.930	0.867
50	1.000	0.915	0.896	0.868	0.839	0.899	0.822
88	1.000	0.911	0.892	0.863	0.834	0.894	0.817

Table 2 OSL signals with the mean and coefficient of variation (COV) for ten replicates of $LiMgPO_4$:Gd phosphors at varying integration times

Integration time (s)	1	2	3	4	5	6	7	8	9	10	Mean	COV
0.1	1.000	0.996	0.993	0.988	0.996	0.987	0.983	0.980	0.978	0.980	0.988	0.79%
0.2	1.000	0.997	0.994	0.991	0.996	0.986	0.985	0.982	0.982	0.979	0.989	0.75%
0.5	1.000	0.994	0.992	0.991	0.993	0.985	0.984	0.981	0.980	0.979	0.988	0.72%
1	1.000	0.996	0.993	0.993	0.995	0.988	0.987	0.984	0.983	0.982	0.990	0.62%
2	1.000	0.997	0.995	0.994	0.996	0.990	0.990	0.987	0.985	0.985	0.992	0.52%
5	1.000	0.997	0.995	0.994	0.996	0.992	0.991	0.988	0.987	0.988	0.993	0.44%
10	1.000	0.997	0.996	0.995	0.997	0.994	0.992	0.990	0.989	0.989	0.994	0.38%
20	1.000	0.998	0.997	0.996	0.997	0.994	0.992	0.991	0.991	0.990	0.995	0.35%
50	1.000	0.998	0.997	0.996	0.997	0.995	0.992	0.991	0.991	0.991	0.995	0.34%
88	1.000	0.998	0.997	0.996	0.998	0.996	0.992	0.991	0.991	0.991	0.995	0.34%

data loss and ensures the preservation of evidence. To satisfy the demand for rapid and multiple readouts, it is necessary to read only a minimal quantity of the OSL signal at any given time. To provide multiple readings, the InLight OSL Reader removes a minimal amount of the OSL signal per reading, with a weak stimulus resulting in a 0.07% reduction and a strong stimulus resulting in a 0.25% reduction [14].

In this study, $LiMgPO_4$:Gd eliminated approximately 2.2% of the OSL signal at each readout, with a readout time of 0.1 s. This method can also be used for multiple readouts. For $LiMgPO_4$:Gd in this study, to eliminate the OSL signal by 0.07% per readout, the stimulus had to be reduced. Relative to TLD-500k, the initial OSL signal, i.e., the sensitivity of the $LiMgPO_4$:Gd phosphor annealed for 1 h at 350 °C with a readout time of 0.1 s, was approximately 0.98, which is sufficient for low-dose measurements in personal, workplace, and environmental dosimetry.

4.2 Fading

The change in the OSL response of an irradiated material over time is referred to as OSL fading. A variety of new OSL materials have been investigated; however, most exhibit severe fading and are not routinely used for dosimetry. OSL signal fading is more difficult to solve than TL signal fading, which is a combination of OSL signals from different traps with different fading characteristics. OSL signal fading cannot be solved by splitting the spectrum into different peaks and removing unstable peaks as in TL signal fading. The problem of OSL signal fading can also be solved by preheating in the same manner as the problem of TL signal fading. However, this approach appears to contradict the premise that the OSL method is suitable for timely processing of a large number of dosimeters. Development of an OSL material that stabilizes the signal over a long period after irradiation is the best approach to solve the problem of OSL signal fading.

The OSL signal fading can be significantly improved by modifying the preparation process. In the case of MgB_4O_7:Ce,Li phosphor, the observed fading of OSL signals following the two preparation processes differed significantly. One study reported that the OSL signals of MgB_4O_7:Ce,Li phosphors exhibited fading of approximately 10–15% over the course of 72 h post-irradiation [55], while another observed that the OSL signals of MgB_4O_7:Ce,Li phosphors synthesized through distinct routes exhibited fading of less than 1% over a period of 40 d [56]. In the case of $LiMgPO_4$:Tb,B, the fading of powder samples was reported to be approximately 20–25% after a period of three weeks following irradiation, although the crystalline samples exhibited a greater degree of fading, exceeding 50% within a period of 24 h following irradiation [42]. For $LiMgPO_4$:Er, the loss of OSL signal intensity after irradiation for 24 h was approximately 40-85% for samples heated to 1000 °C for a period of 2 h, whereas the loss of signal after irradiation for the same duration was below 5% for samples heated to 900 °C for a period of 10 h, when the integration time was above 0.5 s [41]. For $LiMgPO_4$:Gd in this study, the relative residual OSL signals, measured after 24 h of irradiation, ranged from 0.701 to 0.880 for the sample heated for 2 h at 1000 °C. In contrast, the relative residual OSL signals measured after 24 h of irradiation for the other four samples were stable at different integration times. The dependence of the fading on the preparation process was less pronounced for $LiMgPO_4$:Gd than for $LiMgPO_4$:Er.

A reduced number of studies have addressed the relationship between OSL fading and integration time [41]. Signal fading in the $LiMgPO_4$:Er samples was significantly dependent on the integration time. The signal loss in $LiMgPO_4$:Er over a period of 30 d of radiation exposure was reported to be less than 5% when the integration time was greater than 20 s. In contrast, the signal loss on day 30 was approximately 12% when the integration time was 0.1 s [41]. No fading of the OSL signal of $LiMgPO_4$:Gd in this study was observed within 30 days of irradiation when the integration times were less than five seconds, on the 30th day, a total OSL signal fading of approximately 18% was observed. To prevent fading, the integration time (i.e., readout time) of $LiMgPO_4$:Er must be at least 20 s [41]. However, a readout time of 20 s is considerably longer than the typical requirement for a fast OSL readout and is not optimal for multiple readouts. The integration time (i.e., readout time) of $LiMgPO_4$:Gd in this study was as low as 0.1 s, which is sufficient for fast and multiple OSL readouts.

4.3 Superiority of $LiMgPO_4$:Gd

The properties and economics of α-Al_2O_3:C (TLD-500K) and $LiMgPO_4$:Gd are compared in Table 3. Based on the results of this study (Figs. 3b, 4a, and 5f), $LiMgPO_4$:Gd presents no significant advantages over the commercial dosimeter material α-Al_2O_3:C (TLD-500K). With a comparable sensitivity to OSL and an effective atomic number (Table 3) and fading to satisfy fast and multiple measurements,

Table 3 Properties and economics of α-Al_2O_3:C (TLD-500K) and $LiMgPO_4$:Gd

	α-Al_2O_3:C (TLD-500K)	$LiMgPO_4$:Gd
Initial OSL sensitivity	1.000	0.980
Total OSL sensitivity	1.000	0.991
Effective atomic number	11.28	11.44
Manufacturing	Difficulty	Easy
Cost	High	Low

$LiMgPO_4$:Gd has the advantages of easy preparation and low cost.

$LiMgPO_4$:Gd is significantly easier to prepare than α-Al_2O_3:C. One disadvantage of α-Al_2O_3:C is its high melting point (2050 ℃), which presents a challenge for its synthesis, and the harsh growth conditions caused by carbon doping, which can limit its optimization scope. The optimal conditions for the preparation of $LiMgPO_4$:Gd are heating to 900 °C for 15 h.

The growth of carbon-doped alumina crystals is susceptible to fluctuations in the growth conditions, which result in considerable variations in the properties of different parts of the same crystal, as well as between different crystals. To improve the homogeneity of OSL dosimeters, commercially available Luxel+ and InLight OSL dosimeters were produced by blending α-Al_2O_3:C powders with polyester and depositing them on a transparent polyester film. This results in an initial dose that is situated within the linear range of the dose–response curve, exhibiting a considerably inferior response to that of the material itself, which is partly due to the fact that the OSL sensitivity of α-Al_2O_3:C powders is much lower than that of α-Al_2O_3:C crystals. The use of $LiMgPO_4$:Gd for the preparation of dosimeters, such as those of Inlight OSL dosimeters, may confer certain advantages in terms of sensitivity. $LiMgPO_4$:Gd exhibits properties similar to those of Al_2O_3:C. It is easy to synthesize, readily available, inexpensive, and suitable for large-scale production.

5 Conclusions

In this study, five samples of $LiMgPO_4$:Gd phosphor powder were prepared via five different production processes using a solid-state reaction preparation method. X-ray diffraction was used to determine the structures of the five prepared samples. The effects of the preparation process on the OSL decay curves, TL glow curves, OSL sensitivity, MDD, and fading characteristics of the $LiMgPO_4$:Gd phosphors after 24 h of irradiation were investigated. The highest OSL sensitivity was obtained for the $LiMgPO_4$:Gd phosphor heated to 900 °C for 15 h. For the sample heated to 1000 °C for 2 h, the relative residual OSL signals measured after 24 h of irradiation were approximately 0.701−0.88, while the relative residual OSL signals measured after 24 h of irradiation for the other four samples were stable for different integration times. The dependence of fading on the preparation process was found to be less pronounced for $LiMgPO_4$:Gd than for $LiMgPO_4$:Er. Considering its high sensitivity, low fading, and MDD, the $LiMgPO_4$:Gd phosphor heated to 900 °C for 15 h is optimal.

The effect of annealing on OSL sensitivity, relative residual OSL signals measured after 24 h of irradiation, and MDD of $LiMgPO_4$:Gd phosphors heated to 900 °C for 15 h were also investigated. The OSL sensitivity of $LiMgPO_4$:Gd was enhanced by annealing. The $LiMgPO_4$:Gd phosphor annealed at 350 °C for 1 h exhibited the highest OSL sensitivity. For the annealed samples, the OSL signal can be considered stable when the integration time is less than 10 s. The OSL MDD of $LiMgPO_4$:Gd is significantly reduced by annealing. Considering its high sensitivity, low fading, and MDD, annealing at 350 °C for 1 h is optimal.

The basic properties of $LiMgPO_4$:Gd annealed at 350 °C for 1 h were investigated. Over the investigated dose range from 0.1 to 10 Gy, $LiMgPO_4$:Gd phosphors exhibited an excellent linear response. The peak in the TL glow curve of the $LiMgPO_4$:Gd sample represents a first-order phenomenon. E and s were 1.44 eV and 4.82×10^{17} s^{-1}, respectively. The OSL signal of $LiMgPO_4$:Gd was derived from the principal TL glow peak. At a maximum integration time of 5 s, the OSL signal was stable, with no fading 30 d after radiation exposure.

$LiMgPO_4$:Gd eliminated approximately 2.2% of the OSL signal at each readout at a readout time of 0.1 s, which is sufficient for fast and multiple OSL readout. The sensitivity of the $LiMgPO_4$:Gd phosphor annealed for 1 h at 350 °C with a reading time of 0.1 s, was found to be approximately 98% of that observed for TLD-500k, which is sufficient for low-dose measurements in personal, workplace, and environmental dosimetry.

Author contributions All authors contributed to the study conception and design. Material preparation, data collection, and analysis were performed by Kaiyong Tang, Li Fu, Siyuan Zhang, Haijun Fan, Yan Zeng, and Mo Zhou. The first draft of the manuscript was written by Kaiyong Tang, and all authors commented on previous versions of the manuscript. All authors read and approved the final manuscript.

Data availability The data that support the findings of this study are openly available in Science Data Bank at https://cstr.cn/31253.11.sciencedb.j00186.00782 and https://www.doi.org/10.57760/sciencedb.j00186.00782..

Declarations

Conflict of interest The authors declare that they have no Conflict of interest.

References

1. E.G. Yukihara, A.J.J. Bos, P. Bilski et al., The quest for new thermoluminescence and optically stimulated luminescence materials: Needs, strategies and pitfalls. Radiat. Meas. **158**, 106846 (2022). https://doi.org/10.1016/j.radmeas.2022.106846
2. R. Majgier, G. Okada, Optically stimulated luminescence characteristics and dosimetric properties of copper-doped potassium

sulphate. J. Lumin. **257**, 119702 (2023). https://doi.org/10.1016/j.jlumin.2023.119702
3. J. Xu, Z. Chen, M. Gai et al., Fabrication and OSL properties of Eu^{3+}-doped $NaCaPO_4$ glass-ceramics. Mater. Lett. **261**, 126973 (2020). https://doi.org/10.1016/j.matlet.2019.126973
4. J. Zhang, Y. Xiang, C. Wang et al., Recent advances in optical fiber enabled radiation sensors. Sensors **22**, 1126 (2022). https://doi.org/10.3390/s22031126
5. W.S. McKeever, *A Course in Luminescence Measurements and Analyses for Radiation Dosimetry* (West Sussex, John Wiley & Sons Ltd, 2022), pp.1–381
6. H.H. Xiao, L.L. Liu, W.Y. Li et al., TLD calibration and absorbed dose measurement in a radiation-induced liver injury model under a linear accelerator. Nucl. Sci. Tech. **34**, 53 (2023). https://doi.org/10.1007/s41365-023-01211-5
7. Q. Yang, H. Qin, L. Chen et al., Metal-organic framework based thermoluminescence dosimeter. ACS Mater. Lett. **5**, 1619–1626 (2023). https://doi.org/10.1021/acsmaterialslett.3c00326
8. G. Zhang, J. Shen, P. Bao et al., Assessment of occupational exposure of radiation workers at a tertiary hospital in Anhui Province, China, during 2013–18. Radiat. Prot. Dosim. **190**, 237–242 (2020). https://doi.org/10.1093/rpd/ncaa098
9. K. Tang, H. Cui, H. Zhu et al., Study of a new LiF:Mg, Cu, P formulation with enhanced thermal stability and a lower residual TL signal. Radiat. Meas. **42**, 24–28 (2007). https://doi.org/10.1016/j.radmeas.2006.07.001
10. K. Tang, H. Cui, H. Zhu et al., Influence of sintering temperatures on LiF:Mg, Cu, P with various magnesium concentrations. Radiat. Meas. **69**, 7–11 (2014). https://doi.org/10.1016/j.radmeas.2014.07.016
11. S. Zhang, K. Tang, H. Fan et al., A competitive radioluminescence material - LiF:Mg, Cu. P for real-time dosimetry. Radiat. Meas. **151**, 106719 (2022). https://doi.org/10.1016/j.radmeas.2022.106719
12. K. Tang, S. Zhang, Real-time dosimeter based on LiF:Mg, Cu. P and SiPM. Radiat. Meas. **145**, 106607 (2021). https://doi.org/10.1016/j.radmeas.2021.106607
13. X.Y. Zhang, L. Chen, P. Luo et al., TL response of LiF:Mg, Cu, P (GR200A and GR207A) exposed to high-energy ^{12}C ions. Radiat. Meas. **78**, 23–27 (2015). https://doi.org/10.1016/j.radmeas.2014.10.004
14. E.G. Yukihara, S.W.S. McKeever, *Optically Stimulated Luminescence: Fundamentals and Applications* (Elsevier, New York, 2011), pp.1–362
15. E.G. Yukihara, TL and OSL as research tools in luminescence: Possibilities and limitations. Ceram. Int. **49**, 24356–24369 (2023). https://doi.org/10.1016/j.ceramint.2022.10.199
16. C. Termsuk, L. Mitrayon, P. Rindhatayathon et al., Results from 2023 interlaboratory comparison in Southeast and East Asia on OSL personal dosimeter performance in photon fields. Radiat. Meas. **175**, 107181 (2024). https://doi.org/10.1016/j.radmeas.2024.107181
17. X.B. Yang, H.J. Li, Q.Y. Bi et al., Influence of carbon on the thermoluminescence and optically stimulated luminescence of α -Al_2O_3: C crystals. J. Appl. Phys. **104**, 123112 (2008). https://doi.org/10.1063/1.3050344
18. T. Sun, K. Tang, H. Cui et al., Optically stimulated luminescence of α-Al_2O_3: C by the vertical gradient freezing (VGF) method. J. Lumin. **205**, 568–571 (2019). https://doi.org/10.1016/j.jlumin.2018.10.014
19. T. Sun, K. Tang, H. Cui et al., Thermoluminescence of newly developed highly sensitive α-Al_2O_3: C by the vertical gradient freezing method. Radiat. Prot. Dosim. **184**, 174–178 (2019). https://doi.org/10.1093/rpd/ncy196
20. X. Yang, H. Li, Q. Bi et al., Growth of α-Al_2O_3: C crystal with highly sensitive optically stimulated luminescence. J. Lumin. **129**, 566–569 (2009). https://doi.org/10.1016/j.jlumin.2008.12.015
21. X. Yang, J. Xu, H. Li et al., Influence of pulling rates on the thermoluminescence and optically stimulated luminescence of α -Al_2O_3: C crystals grown by the edge-defined, film-fed growth technique. J. Am. Ceram. Soc. **92**(10), 2265–2269 (2009). https://doi.org/10.1111/j.1551-2916.2009.03198.x
22. C.C.P. Fontainha, N. Alves, W.B. Ferraz et al., Very sensitive α -Al_2O_3: C polycrystals for thermoluminescent dosimetry. Appl. Radiat. Isot. **141**, 234–240 (2018). https://doi.org/10.1016/j.apradiso.2018.05.004
23. B. Broadhead, C. Noble, P. Ramachandran, A direct comparison of the optically stimulated luminescent properties of BeO and Al_2O_3 for clinical in-vivo dosimetry. Phys. Eng. Sci. Med. **45**, 859–866 (2022). https://doi.org/10.1007/s13246-022-01155-x
24. W. Abusaid, V. Altunal, Y. Akdeniz et al., Studies of OSL properties of alkali- and rare earth-doped BeO based novel dosimeters for applications in external beam radiotherapy. Radiat. Phys. Chem. **212**, 111136 (2023). https://doi.org/10.1016/j.radphyschem.2023.111136
25. B. Marczewska, A. Sas-Bieniarz, P. Bilski et al., OSL and RL of $LiMgPO_4$ crystals doped with rare earth elements. Radiat. Meas. **129**, 106205 (2019). https://doi.org/10.1016/j.radmeas.2019.106205
26. B. Dhabekar, S.N. Menon, E. Alagu Raja et al., $LiMgPO_4$:Tb, B - A new sensitive OSL phosphor for dosimetry. Nucl. Instrum. Meth. B **269**, 1844–1848 (2011). https://doi.org/10.1016/j.nimb.2011.05.001
27. C. Dotzler, G.V.M. Williams, U. Rieser et al., Optically stimulated luminescence in $NaMgF_3$:Eu^{2+}. Appl. Phys. Lett. **91**(12), 121910 (2007). https://doi.org/10.1063/1.2786599
28. J. Xu, Z. Chen, M. Gai et al., Optically stimulated luminescence of Dy^{3+}-doped $NaCaPO_4$ glass-ceramics. J. Rare Earth **38**, 927–932 (2020). https://doi.org/10.1016/j.jre.2019.05.003
29. Y.H. Wang, H. Chen, F. Chen et al., Radiation dose detection using a high-power portable optically stimulated luminescence real-time reading system. Nucl. Sci. Tech. **29**, 149 (2018). https://doi.org/10.1007/s41365-018-0484-z
30. R. Hemam, L.R. Singh, A.I. Prasad et al., Critical view on TL/OSL properties of $Li_2B_4O_7$ nanoparticles doped with Cu, Ag and co-doping Cu, Ag: Dose response study. Radiat. Meas. **95**, 44–54 (2016). https://doi.org/10.1016/j.radmeas.2016.11.003
31. P.B.R. Gasparian, A.L.M.C. Malthez, E.M. Yoshimura et al., Study of the dosimetric properties of $CaSO_4$:Dy using OSL technique. **17**, P04022 (2022). https://doi.org/10.1088/1748-0221/17/04/P04022
32. V. Guckan, V. Altunal, N. Nur et al., Studying $CaSO_4$: Eu as an OSL phosphor. Nucl. Instrum. Meth. B **407**, 145–154 (2017). https://doi.org/10.1016/j.nimb.2017.06.010
33. J.C. Mittani, M. Prokić, E.G. Yukihara, Optically stimulated luminescence and thermoluminescence of terbium-activated silicates and aluminates. Radiat. Meas. **43**, 323–326 (2008). https://doi.org/10.1016/j.radmeas.2007.10.004
34. A. Jain, A. Tripathi, S. Aggarwal, Thermoluminescence studies of $NaMgF_3$: Tb for gamma dosimetry applications. Nucl. Instrum. Meth. B **543**, 165096 (2023). https://doi.org/10.1016/j.nimb.2023.165096
35. V. Guckan, S.W. Bokhari, V. Altunal et al., Thermoluminescence and optically stimulated luminescence properties of $NaMgF_3$:Dy, Eu synthesized by hydrothermal method and DFT calculations for the bandgap. Mater. Res. Bull. **167**, 112373 (2023). https://doi.org/10.1016/j.materresbull.2023.112373
36. L.C. Oliveira, E. Yukihara, O. Baffa, MgO:Li, Ce, Sm as a high-sensitivity material for optically stimulated luminescence

dosimetry. Sci. Rep-uk. **6**, 24348 (2016). https://doi.org/10.1038/srep24348
37. J. Guo, Q. Tang, C. Zhang et al., Optically stimulated luminescence (OSL) of $LiMgPO_4$:Tm. Tb phosphor. J. Rare Earth **35**, 525–529 (2017). https://doi.org/10.1016/S1002-0721(17)60943-8
38. D.G. Kellerman, M.O. Kalinkin, R.M. Abashev et al., Unusual intrinsic thermoluminescence in $LiMgPO_4$:Er. Chem. Chem. Phys. **22**, 27632–27644 (2020). https://doi.org/10.1039/d0cp05185c
39. D.G. Kellerman, M.O. Kalinkin, D.A. Akulov et al., On the energy transfer in $LiMgPO_4$ doped with rare-earth elements. J. Mater. Chem. C. **9**, 11272–11283 (2021). https://doi.org/10.1039/d1tc02211c
40. M.Q. Gai, Z.Y. Chen, Y.W. Fan et al., Synthesis of $LiMgPO_4$:Eu, Sm, B phosphors and investigation of their optically stimulated luminescence properties. Radiat. Meas. **78**, 48–52 (2015). https://doi.org/10.1016/j.radmeas.2014.09.009
41. L. Fu, K. Tang, S. Zhang et al., Short-term fading studies on optically stimulated luminescence in $LiMgPO_4$:Er. Radiat. Phys. Chem. **218**, 111636 (2024). https://doi.org/10.1016/j.radphyschem.2024.111636
42. D. Kulig, W. Gieszczyk, B. Marczewska et al., Comparative studies on OSL properties of $LiMgPO_4$:Tb. B Powders Crystals. Radiat. Meas. **106**, 94–99 (2017). https://doi.org/10.1016/j.radmeas.2017.04.004
43. Z. Yin, H. Chen, G. Feng et al., Study on the thermoluminescence and optically stimulated luminescence of $LiMgPO_4$: Dy phosphors synthesized by different methods. Appl. Radiat. Isot. **201**, 110990 (2023). https://doi.org/10.1016/j.apradiso.2023.110990
44. M. Gai, Z. Chen, Y. Fan et al., Synthesis and luminescence in $LiMgPO_4$:Tb, Sm, B phosphors with possible applications in real-time dosimetry. J. Rare Earth **31**, 551–554 (2013). https://doi.org/10.1016/S1002-0721(12)60318-4
45. L. Fu, K. Tang, H. Cui et al., The effect of boron co-doping on thermoluminescence and optically stimulated luminescence properties of $LiMgPO_4$:Tb. Sm. Radiat. Meas. **167**, 106986 (2023). https://doi.org/10.1016/j.radmeas.2023.106986
46. H. Tang, L. Lin, C. Zhang et al., High-sensitivity and wide-linear-range thermoluminescence dosimeter $LiMgPO_4$:Tm, Tb, B for detecting high-dose radiation. Inorg. Chem. **58**, 9698–9705 (2019). https://doi.org/10.1021/acs.inorgchem.9b00597
47. L. Fu, H. Cui, H.J. Fan et al., The dependence of thermoluminescence and optically stimulated luminescence properties of $LiMgPO_4$:Tb, Sm, B on maximum heating temperatures. Radiat. Eff. Defect S. **179**, 2294053 (2023). https://doi.org/10.1080/10420150.2023.2294053
48. J. Guo, C. Jian, C. Zeng et al., Dosimetric and spectroscopic study of $LiMgPO_4$ doped with Tm^{3+} and Er^{3+}. RSC Adv. **13**, 4949 (2023). https://doi.org/10.1039/d2ra07109f
49. X. Kong, Z. Fu, H. Que et al., Effects of recording time and residue on dose-response by $LiMgPO_4$:Tb, B ceramic disc synthesized via improved sintering process. Nucl. Instrum. Meth. B **422**, 12–17 (2018). https://doi.org/10.1016/j.nimb.2018.02.032
50. J. Guo, L. Zhao, Q. Tang et al., Spectral study on energy transfer of the $LiMgPO_4$ phosphor doped with Tm^{3+} and Tb^{3+}. J. Lumin. **228**, 117613 (2020). https://doi.org/10.1016/j.jlumin.2020.117613
51. A.L.M.C. Malthez, B. Marczewska, D. Kulig et al., Optical and thermal pre-readout treatments to reduce the influence of fading on $LiMgPO_4$ OSL measurements. Appl. Radiat. Isot. **136**, 118–120 (2018). https://doi.org/10.1016/j.apradiso.2018.02.022
52. L. Fu, K. Tang, S. Zhang et al., Fading performance on optically stimulated luminescence of $LiMgPO_4$:Tb, Sm. B. Radiat. Meas. **175**, 107165 (2024). https://doi.org/10.1016/j.radmeas.2024.107165
53. S.N. Menon, B.S. Dhabekar, S. Kadam et al., Fading studies in $LiMgPO_4$:Tb, B and synthesis of new $LiMgPO_4$ based phosphor with better fading characteristics. Nucl. Instrum. Meth. B **436**, 45–50 (2018). https://doi.org/10.1016/j.nimb.2018.08.052
54. R. Chen, On the calculation of activation energies and frequency factors from glow curves. J. Appl. Phys. **40**, 570–585 (1969). https://doi.org/10.1063/1.1657437
55. E.G. Yukihara, B.A. Doull, T. Gustafson et al., Optically stimulated luminescence of MgB_4O_7:Ce, Li for gamma and neutron dosimetry. J. Lumin. **183**, 525–532 (2017). https://doi.org/10.1016/j.jlumin.2016.12.001
56. L.F. Souza, A.M.B. Silva, P.L. Antonio et al., Dosimetric properties of MgB_4O_7:Dy, Li and MgB_4O_7:Ce, Li for optically stimulated luminescence applications. Radiat. Meas. **106**, 196–199 (2017). https://doi.org/10.1016/j.radmeas.2017.02.009